# **ORGANOMETALLICS**

pubs.acs.org/Organometallics Article

# Electronic Rearrangement in Steps of Reductive Elimination of Polar Electrophiles Leads to Refinement of Redox Events

Kevin Basemann,\* Jennifer J. Becker, Theresa L. Windus, and Michel R. Gagné\*



Cite This: Organometallics 2023, 42, 2171–2176



**ACCESS** I

Metrics & More

Article Recommendations

Supporting Information

**ABSTRACT:** The oxidative addition/reductive elimination of polar molecules such as methyl iodide at late metal centers has a strongly supported  $S_N2$  mechanism for many key organometallic complexes, including important industrial catalysts. In the reductive elimination direction, it is proposed that a ligand initially dissociates, typically a halide, followed by subsequent nucleophilic attack at the ligand trans to the now vacant site. The prevailing view is the metal reduction occurs upon transferring the electrophile in the  $S_N2$  step. Herein, we report the use of an

ensemble of computational techniques to characterize the electronic structure of the reactants and intermediates along this reductive elimination pathway. These calculations demonstrate, unexpectedly, that the initiating loss of an anionic ligand from the octahedral highly oxidized structure leads to an electronic rearrangement that shifts electron density from the apical ligand back toward the metal resulting in an inversion of the electron flow between the metal and apical ligand. The anisotropic shift in electron density to the metal disproportionately affects the apical position, which is best described as a Pt  $\rightarrow$  Me dative bond. With this Pt  $\rightarrow$  Me bonding description, our interpretation of the IUPAC oxidation state formalism would assign the intermediate as Pt<sup>II</sup>. Although counterintuitive, the formal and functional reduction of the metal thus occurs upon halide dissociation.

# **■ INTRODUCTION**

The oxidative addition/reductive elimination of polar molecules at metal centers is an essential reaction in organometallic chemistry and a critical step in numerous large-scale industrial processes. The mechanism of nucleophilic reductive elimination or the microscopic reverse, oxidative addition, has been studied for a wide variety of complexes, particularly complexes of Rh, Ir, and Pt. The Monsanto and Cativa processes undergo a nucleophilic reductive elimination of acetyl iodide as well as an oxidative addition of methyl iodide in key steps of their catalytic cycles (Scheme 1A). Some classic complexes and catalysts, including Vaska's complex  $^{4,11-13}$  and the Shilov system, undergo oxidative addition or reductive elimination of polar molecules via  $\rm S_{N}2$ -like mechanisms. Perhaps, the most studied example of the  $\rm S_{N}2$  oxidative addition/reductive elimination reaction comes from Goldberg.  $^{8,16,17}$ 

The two-step reductive elimination of methyl iodide from  $(dppe)PtMe_3I$  (dppe=1,2-bis(diphenylphosphino)ethane) and corresponding reverse,  $S_N2$  oxidative addition of methyl iodide to  $(dppe)PtMe_2$ , is covered in several organometallic textbooks as it is representative of a broad class of redox reactions wherein a polar reagent oxidatively adds to a metal center and becomes activated. The reductive elimination direction occurs over two steps, with the first being iodide dissociation to form a common cationic platinum intermediate  $(B, Scheme\ 1B)$ , which is susceptible to iodide attack at the methyl group trans to the now vacant site on the metal center.

As shown in Scheme 1B, the five-coordinate intermediate reacts by nucleophilic attack of I<sup>-</sup> at the apical methyl position, obviously, implying this methyl group is electrophilic. In this case, the traditional description of the Pt<sup>+</sup>/Me<sup>-</sup> bond and its reactivity diverge. A preponderance of reductive elimination mechanisms in octahedral geometries ascribe a special reactivity to (and need for) the five-coordinate intermediate. It is conceivable that the square pyramidal geometry is somehow enabling electrophilic reactivity by virtue of microscopic reversibility considerations or by an electronic structure bias, or both.

Our study began with a careful charge analysis of intermediate **B** (Table 1). As will be discussed, iodide loss dramatically alters the apical methyl group, inverting its charge from negative in **A** ( $\sim$ -0.15) to positive in **B** ( $\sim$ +0.15). In addition to being consistent with observed reactivity, this change suggested a more extreme description, namely, a reverse dative interaction between Pt and Me, i.e., Pt  $\rightarrow$  Me. The divergence of this description from a more conventional formalism prompted a

Received: February 20, 2023 Published: August 11, 2023





Organometallics pubs.acs.org/Organometallics Article

Scheme 1. (A) Monsanto Process for the Synthesis of Acetic Acid; (B) Reversible Mechanism of Addition/Elimination of MeI to (dppe)PtMe<sub>2</sub>

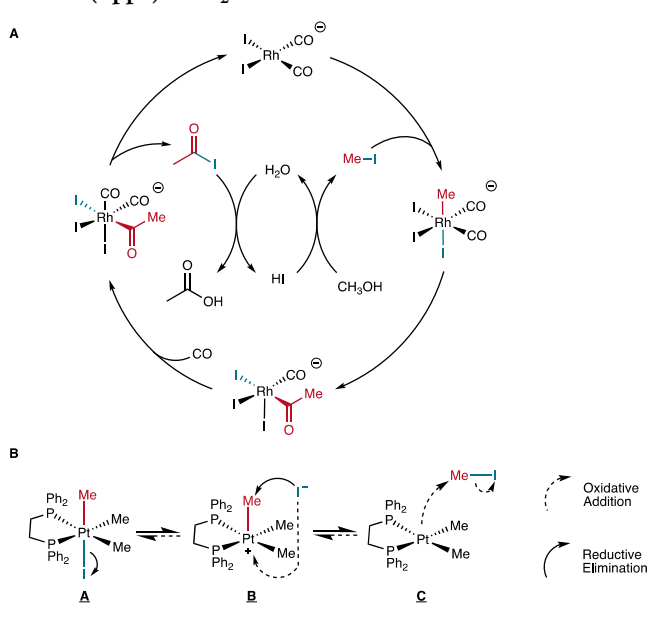


Table 1. Bader Charge Analysis at Various Levels of Theory

<u> </u>	Me <sub>2</sub>	e +l	Pr + M	e +Me+	Me <sub>2</sub>	Me
	A		<u>B</u>		<u>C</u>	
theory	A, Pt	A, Me <sup>1</sup>	A, Me <sup>2</sup>	B, Pt	B, Me <sup>1</sup>	B, Me <sup>2</sup>
1	0.35	-0.10	-0.16	0.31	0.13	-0.12
2	2.19	-0.11	-0.18	1.84	0.11	-0.14
3	0.42	-0.14	-0.18	0.42	0.11	-0.14
4	0.60	-0.15	-0.22	0.54	0.13	-0.19
5	0.35	-0.05	-0.21	0.35	0.13	-0.17
6	0.30	-0.09	-0.15	0.27	0.13	-0.11
7	0.30	-0.09	-0.16	0.26	0.15	-0.12
8 <sup>b</sup>	0.37	-0.15	-0.20	0.36	0.11	-0.16

"Level of theory definitions: (1) M06-2X/Def2-TZVP(H,C,P,I)/SDD(Pt), (2) M06-2X/Def2-TZVP(H,C,P)/Sapporo-TZP(Pt,I)/Douglas—Kroll—Hess, (3) B3LYP/Def2-TZVP(H,C,P,I)/SDD(Pt), (4) HF/Def2-TZVP(H,C,P,I)/SDD(Pt), (5) M06-2X/Def2-TZVP-(H,C,P,I)/SDD(Pt)/COSMO(acetone), (6) M06-2X/6-311++G\*\*(H,C,P)/Def2-TZVP(I)/SDD(Pt), (7) M06-2X/aug-CC-pVQZ(H,C,P)/Def2-TZVP(I)/SDD(Pt), (8) wB97X/Def2-TZVP-(H,C,P,I,Pt). \*\*Bader charge analysis performed with Multiwfn 3.7.

series of additional electronic structure calculations specifically focused on the nature of the Pt—Me bond.

The energy decomposition analysis (EDA) and localized orbital bonding analysis (LOBA) methods together (vide infra) revealed a structure wherein the apical Pt—Me bond in  ${\bf B}$  is a Pt  $^{\rm II}$   $\rightarrow$  Me reverse dative bond and the equatorial Pt—Me bonds are more traditional by every measure. Consequently, the electronic structure calculations support a situation wherein  ${\bf B}$  is significantly reduced (Pt  $^{\rm II}$ ) and the apical ligand is significantly positive. This flow of electron density in  ${\bf A}$  from the apical Me ligand to the metal fragment on the loss of the trans  ${\bf I}^-$  suggests that the actual metal redox step is intraligand and occurs upon iodide loss.

## RESULTS AND DISCUSSION

Charge Analysis. The Goldberg mechanism of methyl iodide loss from (dppe)PtMe<sub>3</sub>I was investigated to probe the electronic structure of the key complexes in reductive elimination. Our initial calculations sought to understand how electronic populations around platinum and its ligands changed with the removal of iodide in a system analogous to (dppe)PtMe<sub>3</sub>I. For computational ease, we focused on (dmpe)- $PtMe_3I$  (dmpe = 1,2-bis(dimethylphosphino)ethane). Optimization and subsequent charge analysis of the octahedral (dmpe)PtMe<sub>3</sub>I (A) and cationic five-coordinate (dmpe)PtMe<sub>3</sub><sup>+</sup> (B) were performed. Somewhat surprisingly, Bader <sup>18,19</sup> charge analysis revealed that the charge at platinum in cationic **B** was less positive than that of A. This observation ran counter to our expectations as a cationic, coordinatively unsaturated PtIV complex would logically carry a more positively charged metal center than a neutral Pt<sup>IV</sup> complex, particularly with platinum as the most electropositive atom in the molecule. It is important to state that these calculated charges/electronic population analyses do not reflect oxidation state or formal charge and as expected the total charge is delocalized over the entire molecule. As a result, the computed differences in charge at Pt are quite small. The noteworthy factor in this analysis is that the positive charge on platinum decreased after loss of an anionic ligand suggesting, paradoxically, that electron density increased around platinum on loss of iodide. Further analysis of the charges revealed negligible changes in each of the equatorial atoms directly bound to platinum; however, the apical methyl now carried a more positive charge in B than in A. This is not to say that other atoms in the molecule do not change their charge, but the most significant increase in positive charge occurs in the apical methyl group. Given the unexpected result of these calculations, we were skeptical of the robustness of the computational methodology, so calculations were repeated with multiple independent factors considered. The charge trends remain consistent for different density functionals or wavefunction methods (level of theory 1, 3, 4, 8), using an allelectron basis set with Douglas-Kroll relativistic treatment (level of theory 2, note this all-electron treatment leads to a larger magnitude of charge on platinum, but if measured based off the relative number of electrons included in the basis set it is in line with other levels of theory discussed), and use of different basis sets (level of theory 1, 6, 7). From the lowest to the highest levels of theory, the trend of the platinum center being less positive or unchanged and the apical methyl more positive in charge on going from A to cationic B was consistent (Table 1). As has been discussed in previous articles, charge and oxidation states are not the same, and it would be inappropriate to conclude from this analysis any change in the oxidation state.<sup>20</sup> Similarly, this does not suggest that there is an inversion of bond polarity as platinum remains more positively charged than the apical methyl group. However, the analysis does lead to the conclusion that iodide loss causes an increase in electron density at the metal center and a decrease in electron density at the apical methyl group. Moreover, the bulk of the changes are in the apical and not in the equatorial methyl groups.

**Electron Density Analysis.** To better illustrate the electronic changes in A vs B, an electron density difference plot was made using MacMolPlt (Figure 1).<sup>21</sup> This was accomplished by taking the difference in electron density between a fully optimized calculation of A and the same structure with the  $I^-$  ligand excised (i.e., unoptimized B). This

Organometallics pubs.acs.org/Organometallics Article

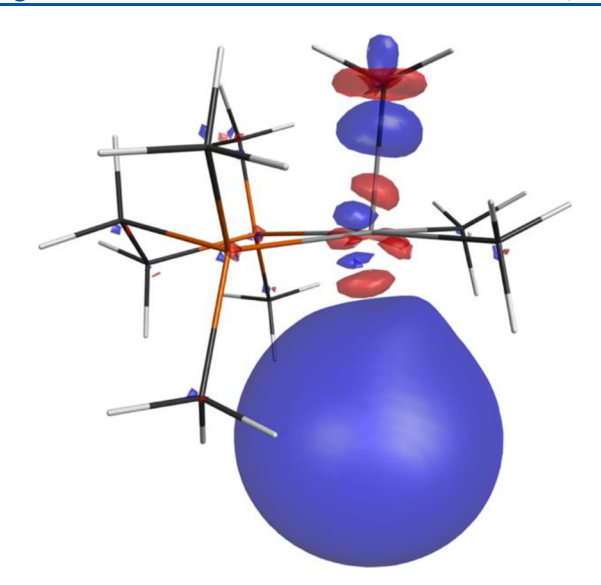


**Figure 1.** Electron density difference map between **A** and an unoptimized cationic five-coordinate platinum species (see text). Blue depicts a loss of electron density; red depicts an increase in electron density. The large blue portion at the bottom of the figure is the result of  $I^-$  removal from **A**.

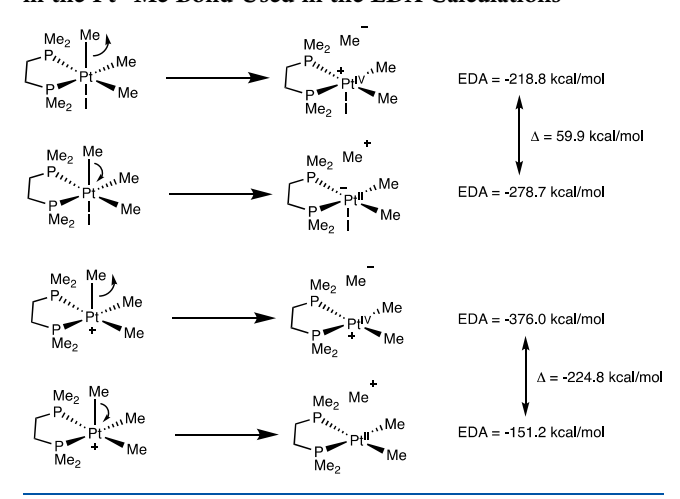
approach maximized atomic overlap between calculations and focused the visualization. This subtractive analysis creates an inconsequential large void of electron density (blue) in the original position of the I. More illustrative are the remaining blue and red regions, which report on changes in electron density accompanying iodide loss. The total electron density around the platinum center has increased after the loss of iodide (more red than blue), while the electron density around the apical carbon has decreased (more blue than red); all other atoms in the system remained largely unchanged. Clearly, there are regions of electron density gain and loss in both platinum and the apical carbon, and the shape of the gain and loss is directed along z, suggestive of some change of polarization upon loss of iodide. This analysis is related to the conclusions discussed in the Bader charge analysis and better supports the notion that loss of iodide increases the electron density at platinum.

Electron Flow/Energy Decomposition Analysis. The results of the charge/population analysis suggested that a view of the apical Pt-Me as a purely covalently bonded unit was insufficiently nuanced. Since the above Bader analysis only yielded information about charges/electron population, a third approach was used to compare the electron configurations of A and B. Energy decomposition analysis (EDA) enables one to calculate the energy of interacting a ligand (L) with the rest of the compound (M)<sup>22</sup> within a geometry-optimized structure. Splitting the electrons of the bond to sit either on the ligand  $(L^{-}/M^{+})$  or the metal fragment  $(L^{+}/M^{-})$  allows one to compute interaction energies for both (extreme) heterolytic forms of the M-L bond. The smaller of the two energies corresponds to the L-M bond's more favorable heterolytic splitting direction. The difference between the two interaction energies additionally provides a semiquantitative measure of this preference. It is important to note what EDA values are not. First, they do not provide oxidation state information as different ligands on the same molecule can give different heterolytic cleavage preferences, and second, they are not a bond dissociation energy. This methodology was inspired by the work of Frenking et al. in their similar application of EDA-NOCV methods for evaluating

bonds.<sup>23</sup> Frenking used the term electron flow to describe whether an M-L was best described as  $M \to L$  or  $L \to M$ .

Our implementation of this technique performed two EDA calculations, splitting 2 electrons to either sit on the apical methyl group or on platinum for both  $\bf A$  and  $\bf B$ . The outcome is a preference for either the  $Pt^{II}/Me^+$  or the  $Pt^{IV}/Me^-$  interpretation of the electron splitting (Scheme 2). Unsurprisingly,

Scheme 2. Depiction of the Two Modes of Electron Splitting in the Pt—Me Bond Used in the EDA Calculations



octahedral **A** preferred the Pt<sup>IV</sup>/Me<sup>-</sup> configuration by 59.9 kcal/mol. The same analysis of cationic **B** unexpectedly revealed the apical Pt<sup>II</sup>/Me<sup>+</sup> combination to be preferred by 224.8 kcal/mol. EDA calculations consequently reveal that the electron flow of the apical Pt–Me bond is inverted upon converting **A** to **B**.

While we have depicted/described this as an oxidation state change on platinum, it is important to reiterate that electron splitting in the EDA calculations places the electrons on the entire fragment, i.e., CH<sub>3</sub> or (dmpe)PtMe<sub>2</sub>I, and these two electrons cannot be distinguished as sitting on any single atom in either fragment. The preference for **B** to localize positive charge on the apical methyl group rather than potentially being distributed on platinum and the multiple other ligands in that fragment is noteworthy and suggests that electrons, upon iodide loss, flow from the apical CH<sub>3</sub> - ligand to the metal center rather than away from it. In contrast, if an equatorial methyl group is put through the same analysis, the preference is for the fragmentation to prefer the traditional Pt<sup>IV</sup>/Me<sup>-</sup> configuration. To be clear, this is not in contention with our results with the apical methyl group assignment (favored Pt<sup>II</sup>/Me<sup>+</sup>), as this is not a method for assigning oxidation states, but rather demonstrates the preferred heterolytic fragmentation of that bond in particular. The diversity of electron flow changes reinforces the notion that a dogmatic view of B does not capture the polarized apical Pt -> Me reverse dative bond implied by computation. Due to some criticism of the EDA methodology used in this context, we have also calculated the fragments of this heterolytic bond cleavage and determined the same results, namely that the PtII/Me+ fragmentation direction is the more favored in the five-coordinate species.

**Localized Orbital Bonding Analysis.** The consistency of the  $Pt^{II} \rightarrow Me^+$  bond formulation across the various methods led us to shift our analysis to directly assessing the oxidation state of platinum in **B**. The localized orbital bonding analysis (LOBA) method was previously developed to assess the oxidation state of transition metal compounds, <sup>24</sup> and while the LOBA method

**Organometallics** pubs.acs.org/Organometallics Article

does not give a single unique answer to the oxidation state, it has been utilized to assign or confirm oxidation states for a wide variety of compounds including difficult and nonobvious oxidation states such as transition metal oxo species and around transition metals with redox noninnocent ligands. 25,26 The approach examines localized MOs and applies an electron population analysis analogous to the Bader analysis to assign these localized orbitals to an atom. Key to the LOBA analysis is the choice of a threshold at which an orbital is considered localized on a given atom. In works exploring this concept, it has been found that the appropriate threshold value can vary, but it has generally been concluded that a threshold value of  $\sim$ 50% is reliable.24,2

The LOBA method was utilized with a few localization methods, Pipek-Mezey<sup>28</sup> and Fosters-Boys,<sup>29</sup> using a threshold value of 50% (see SI for extended analysis). The LOBA method was used on a variety of calculations using both ECPs and all-electron relativistic methods for both A and B. In each case, the six-coordinate A returns a PtIV outcome, while the cationic five-coordinate B is in the PtII oxidation state. The LOBA results are therefore fully consistent with EDA and electron density calculations and suggest a Pt<sup>II</sup> oxidation state for B. These outcomes are ultimately a consequence of a significant shift in electron density from the apical CH3 to Pt on loss of iodide from A.

Qualitative Molecular Orbital Analysis. To state the obvious, these data run counter to the traditional view of oxidative addition/reductive elimination of polar reagents around late metal centers. The above calculations indicate that it is the dissociation of an anionic ligand, iodide, which triggers an electron density enhancing reduction of the metal center. Approaching this sequence from the microscopic reverse of oxidative addition and assessing the involved molecular orbitals provides a useful perspective. In the oxidative addition of methyl iodide to square planar (dppe)PtMe2, the mechanism is widely agreed to first involve nucleophilic addition of the Pt center along z to the electrophilic methyl iodide. 1,2 From this formulation, an MO diagram can be constructed rationalizing why a Pt<sup>II</sup> oxidation state is not unreasonable (Scheme 3). The filled d<sub>2</sub><sup>2</sup> is the highest occupied molecular orbital (HOMO) of (dppe)PtMe2 for the nucleophilic attack on the lowest unoccupied molecular orbital (LUMO) of methyl iodide, as

Scheme 3. MO Diagram Describing the Interaction of a Square Planar PtII Species with Methyl Iodide To Form the Five-Coordinate Intermediate

confirmed by calculation of the two species individually. Since unoccupied orbitals are inherently higher in energy than occupied MOs, the new bonding molecular orbital consequently has more platinum character, and the new antibonding orbital has more methyl character (Scheme 3). Understandably, a filled MO with more Pt character would tend to localize those electrons on Pt, i.e., more PtII character.

This MO argument and each computational method brought to bear on the electronic structure of **B** support the notion that the apical methyl ligand is an  $M \rightarrow L$  dative bond. The modified IUPAC rules for assigning oxidation states<sup>30</sup> consequently lead to a Pt<sup>II</sup> assignment for **B**. In the reductive elimination direction, this indicates that the reduction of Pt<sup>IV</sup> actually begins upon iodide dissociation and not upon loss of Me+. This view, which in the microscopic reverse suggests that the oxidation state of platinum does not functionally (and formally since the apical Me is an  $M \to L$  dative bond) increase from  $Pt^{II}$  to  $Pt^{IV}$  until iodide coordination, reveals nonobvious redox triggers.

**Other Compounds.** To determine whether this outcome reflected a broader phenomenon in organometallic chemistry, the same methodologies were applied to several other complexes with important historical or practical utility. A more electronpoor system was explored in the reductive elimination of MeI from the PMe<sub>3</sub> version of Vaska's complex (Scheme 4A). In the

Scheme 4. (A) Iodide Dissociation from Iridium in a Model for Vaska's Complex; (B) Iodide Dissociation in the Monsanto Acetic Acid Catalyst; and (C) Chloride Dissociation in the Shilov System

A 
$$OC$$
,  $Me_3$   $PMe_3$   $OC$ ,  $Me_3$   $OC$ ,  $Me_4$   $OC$ ,  $Me_4$   $OC$ ,  $Me_5$   $OC$ ,  $Me5$   $OC$ ,  $Me5$ 

reductive elimination direction, the charge on iridium was unchanged upon iodide dissociation from octahedral Ir<sup>III</sup>. This lack of positive charge buildup upon generating a cationic structure reinforces the notion of a flow of electron density from the remaining ligands to the metal center, particularly the apical methyl ligand. Like the Goldberg system, EDA and LOBA calculations additionally suggest that the five-coordinate structure is  $Ir^I$  with an apical  $M \to Me$  datively bound, i.e., iodide dissociation triggered an Ir<sup>III</sup> to Ir<sup>I</sup> reduction. Similar outcomes were obtained with other d<sup>6</sup>/d<sup>8</sup> catalytically relevant complexes. For example, the Rh<sup>I</sup>/Rh<sup>III</sup> and related Ir<sup>I</sup>/Ir<sup>III</sup> catalysts are responsible for generating 60% of global acetic acid (Monsanto and Cativa processes, Scheme 4B)<sup>31</sup> and the proposed intermediate of the well-studied Shilov system (Scheme 4C) both showed a decrease in positive charge at the

Organometallics pubs.acs.org/Organometallics Article

metal upon loss of an anionic ligand. In both cases, EDA and LOBA studies showed that loss of the trans anionic ligand triggered a functional, and formal, metal reduction.

# CONCLUSIONS

Our analysis provides insight into the sequence of electronic structure changes accompanying the stepwise reductive elimination of small molecules from multiple d<sup>6</sup>/d<sup>8</sup> textbook complexes. Computational analysis of the charge at a series of octahedral metal centers revealed that loss of an anionic iodide (or chloride) ligand triggered an increase in the metal's electron density at the expense of the trans axial ligand, enough to consider the apical Pt–Me bond to be a Pt  $\rightarrow$  Me dative bond. The IUPAC definition for assigning oxidation state is therefore relevant: "oxidation state equals the charge of an atom after its homonuclear bonds have been divided equally and heteronuclear bonds assigned to the bond partners according to Allen electronegativity, except when the electronegative atom is bonded reversibly as a Lewis-acid ligand, in which case it does not obtain that bond's electrons."30 Although it is debatable what constitutes a reversibly bound Lewis acid ligand (CH<sub>3</sub><sup>+</sup> loss is clearly unfavorable but a more stabilized carbocation could be, e.g., Gabbai et al.<sup>32</sup>), a series of characterization methods describing the key bond as  $Pt \rightarrow Me$  implies an alignment to the IUPAC description. If one accepts the argument (and data) that the CH<sub>3</sub> ligand is a Lewis acid, then both the IUPAC formalism and the LOBA analysis indicate the metal has been functionally and formally reduced upon dissociation of I-. Even if one does not accept the argument of reversibility, the data clearly demonstrate a Lewis acid apical ligand in the five-coordinate intermediates. Finally, the root cause of the inversion of electron flow along z in the studied five-coordinate structures is ultimately the empty coordination site. More than just a potential position to coordinate a ligand, the electronic perturbation caused by this vacancy creates the electrophilicity along z. The potential for altering fundamental reactivity in this manner is the subject of current efforts.<sup>33</sup>

## ASSOCIATED CONTENT

# Supporting Information

The Supporting Information is available free of charge at https://pubs.acs.org/doi/10.1021/acs.organomet.3c00102.

Cartesian coordinates for all calculations used in this work (XYZ)

Computational methodology, additional data and analysis of charge, energy decomposition analysis, and LOBA calculations (PDF)

# AUTHOR INFORMATION

# **Corresponding Authors**

Kevin Basemann — Caudill Laboratories, Department of Chemistry, University of North Carolina at Chapel Hill, Chapel Hill, North Carolina 27599, United States; orcid.org/0000-0001-8203-0112; Email: kbasemann@unc.edu

Michel R. Gagné — Caudill Laboratories, Department of Chemistry, University of North Carolina at Chapel Hill, Chapel Hill, North Carolina 27599, United States; orcid.org/0000-0001-8424-5547; Email: mgagne@unc.edu

#### **Authors**

Jennifer J. Becker — U.S. Army Research Office, Research Triangle Park, North Carolina 27709, United States Theresa L. Windus — Ames Laboratory, Ames, Iowa 50011, United States; Department of Chemistry, Iowa State University, Ames, Iowa 50011, United States; orcid.org/ 0000-0001-6065-3167

Complete contact information is available at: https://pubs.acs.org/10.1021/acs.organomet.3c00102

#### **Notes**

The authors declare no competing financial interest.

# ACKNOWLEDGMENTS

K.B. thanks the National Research Council for Postdoctoral Fellowship, and M.R.G. thanks the National Science Foundation for support (CHE-2154432). T.L.W. thanks funding through the U.S. Department of Energy, Office of Science, Basic Energy Sciences, Division of Chemical Sciences, Geosciences, and Biosciences through the Ames Laboratory Computational and Theoretical Chemistry program. We thank the University of North Carolina at Chapel Hill and the Research Computing group for providing computational resources and support that have contributed to these research results. We would like to thank Professor Josef Takats for helpful discussions on this work. Finally, we thank the referees for their critical readings and their numerous suggestions for solidifying the arguments outlined herein.

# REFERENCES

- (1) Hartwig, J. F. Reductive Eliminations. In *Organotransition Metal Chemistry From Bonding to Catalysis*; University Science Books, 2010; pp 321–348.
- (2) Crabtree, R. H. Oxidative Addition and Reductive Elimination. In The Organometallic Chemistry of the Transition Metals; Wiley, 2009; pp 153–176
- (3) Nabavizadeh, S. M.; Habibzadeh, S.; Rashidi, M.; Puddephatt, R.J. Oxidative Addition of Ethyl Iodide to a Dimethylplatinum(II) Complex: Unusually Large Kinetic Isotope Effects and Their Transition-State Implications. *Organometallics* **2010**, *29*, 6359–6368.
- (4) Chock, P. B.; Halpern, J. Kinetics of the Addition of Hydrogen, Oxygen, and Methyl Iodide to Some Square-Planar Iridium(I) Complexes 1. J. Am. Chem. Soc. 1966, 88, 3511–3514.
- (5) Crespo, M.; Puddephatt, R. J. Cationic Intermediates in Oxidative Addition Reactions of Alkyl Halides to D8 Complexes: Evidence for the  $S_{\rm N}2$  Mechanism. *Organometallics* **1987**, *6*, 2548–2550.
- (6) Griffin, T. R.; Čook, D. B.; Haynes, A.; Pearson, J. M.; Monti, D.; Morris, G. E. Theoretical and Experimental Evidence for  $S_N 2$  Transition States in Oxidative Addition of Methyl Iodide to Cis $[M(CO)_2I_2]^-$  (M = Rh, Ir). J. Am. Chem. Soc. 1996, 118, 3029–3030. (7) Gaunt, J. A.; Gibson, V. C.; Haynes, A.; Spitzmesser, S. K.; White, A. J. P.; Williams, D. J. Bis(Imino)Carbazolide Complexes of Rhodium: Highly Nucleophilic Ligands Exerting a Dramatic Accelerating Effect on MeI Oxidative Addition. Organometallics 2004, 23, 1015–1023.
- (8) Goldberg, K. I.; Yan, J. Y.; Winter, E. L. Competitive Carbon-Carbon Reductive Elimination and Carbon-Iodide Bond Formation from a Pt(IV) Complex. J. Am. Chem. Soc. 1994, 116, 1573–1574.
- (9) Hickey, C. E.; Maitlis, P. M. Oxidative Addition of Methyl Lodide to Dicarbonylrhodium(I) Complexes. *J. Chem. Soc., Chem. Commun.* **1984**, 23, 1609.
- (10) Forster, D. Kinetic and Spectroscopic Studies of the Carbonylation of Methanol with an Iodide-Promoted Iridium Catalyst. *J. Chem. Soc., Dalton Trans.* **1979**, *11*, 1639.
- (11) Stang, P. J.; Schiavelli, M. D.; Chenault, H. K.; Breidegam, J. L. Kinetic Deuterium Isotope Effects in the Reaction of Vaska's

**Organometallics** Article pubs.acs.org/Organometallics

Compound (Ph<sub>3</sub>P)<sub>2</sub>Ir(CO)Cl with Methyl Iodide and MeOSO2CF3. Organometallics 1984, 3, 1133-1134.

- (12) Stieger, H.; Kelm, H. Effect of Solvent and Pressure on the Rates of the Oxidative Addition Reactions of Methyl Iodide and Oxygen to Chlorocarbonylobis(Triphenylphosphine)Iridium(I). J. Phys. Chem. 1973, 77, 290-294.
- (13) Thompson, W. H.; Sears, C. T. Kinetics of Oxidative Addition to Iridium(I) Complexes. Inorg. Chem. 1977, 16, 769-774.
- (14) Eisenstein, O.; Crabtree, R. H. Functionalization vs.  $\beta$ -Elimination in Alkane Activation: A Key Role for 16-Electron ML<sub>5</sub> Intermediates. New J. Chem. 2001, 25, 665-666.
- (15) Luinstra, G. A.; Wang, L.; Stahl, S. S.; Labinger, J. A.; Bercaw, J. E. C-H Activation by Aqueous Platinum Complexes: A Mechanistic Study. J. Organomet. Chem. 1995, 504, 75-91.
- (16) Williams, B. S.; Holland, A. W.; Goldberg, K. I. Direct Observation of C-O Reductive Elimination from Pt(IV). J. Am. Chem. Soc. 1999, 121, 252-253.
- (17) Goldberg, K. I.; Yan, J.; Breitung, E. M. Energetics and Mechanisms of Carbon-Carbon and Carbon-Iodide Reductive Elimination from a Pt(IV) Center. J. Am. Chem. Soc. 1995, 117, 6889-6896.
- (18) Henkelman, G.; Arnaldsson, A.; Jónsson, H. A Fast and Robust Algorithm for Bader Decomposition of Charge Density. Comput. Mater. Sci. 2006, 36, 354-360.
- (19) Bader, R. F. W. Atoms in Molecules: A Quantum Theory; Oxford University Press: New York, 1990.
- (20) Parkin, G. Valence, Oxidation Number, and Formal Charge: Three Related but Fundamentally Different Concepts. J. Chem. Educ. 2006, 83, 791.
- (21) Bode, B. M.; Gordon, M. S. Macmolplt: A Graphical User Interface for GAMESS. J. Mol. Graphics Modell. 1998, 16, 133-138.
- (22) Su, P.; Li, H. Energy Decomposition Analysis of Covalent Bonds and Intermolecular Interactions. J. Chem. Phys. 2009, 131, No. 014102.
- (23) Bickelhaupt, F. M.; Fonseca Guerra, C.; Mitoraj, M.; Sagan, F.; Michalak, A.; Pan, S.; Frenking, G. Clarifying Notes on the Bonding Analysis Adopted by the Energy Decomposition Analysis. Phys. Chem. Chem. Phys. 2022, 24, 15726-15735.
- (24) Thom, A. J. W.; Sundstrom, E. J.; Head-Gordon, M. LOBA: A Localized Orbital Bonding Analysis to Calculate Oxidation States, with Application to a Model Water Oxidation Catalyst. Phys. Chem. Chem. Phys. 2009, 11, 11297-11304.
- (25) Thenarukandiyil, R.; Paenurk, E.; Wong, A.; Fridman, N.; Karton, A.; Carmieli, R.; Ménard, G.; Gershoni-Poranne, R.; de Ruiter, G. Extensive Redox Non-Innocence in Iron Bipyridine-Diimine Complexes: A Combined Spectroscopic and Computational Study. Inorg. Chem. 2021, 60, 18296-18306.
- (26) Sun, D.; Wu, Z.; Zhang, X.; Yang, J.; Zhao, Y.; Nam, W.; Wang, Y. Brønsted Acids Promote Olefin Oxidations by Bioinspired Nonheme Co<sup>III</sup>(PhIO)(OH) Complexes: A Role for Low-Barrier Hydrogen Bonds. J. Am. Chem. Soc. 2023, 145, 5739-5749.
- (27) Gimferrer, M.; van der Mynsbrugge, J.; Bell, A. T.; Salvador, P.; Head-Gordon, M. Facing the Challenges of Borderline Oxidation State Assignments Using State-of-the-Art Computational Methods. Inorg. Chem. 2020, 59, 15410-15420.
- (28) Pipek, J.; Mezey, P. G. A Fast Intrinsic Localization Procedure Applicable for ab initio and Semiempirical Linear Combination of Atomic Orbital Wave Functions. J. Chem. Phys. 1989, 90, 4916-4926.
- (29) Foster, J. M.; Boys, S. F. Canonical Configurational Interaction Procedure. Rev. Mod. Phys. 1960, 32, 300-302.
- (30) Karen, P.; McArdle, P.; Takats, J. Comprehensive Definition of Oxidation State (IUPAC Recommendations 2016). Pure Appl. Chem. 2016, 88, 831-839.
- (31) Beller, M.; Wu, X.-F. Transition Metal Catalyzed Carbonylation Reactions; Springer Berlin Heidelberg: Berlin, Heidelberg, 2013.
- (32) Litle, E. D.; Gabbaï, F. P. A Cationic Gold-Fluorenyl Complex with a Dative AuC+ Bond: Synthesis, Structure, and Carbophilic Reactivity. Chem. Commun. 2023, 59, 603-606.

(33) Neff, K. R.; Basemann, K.; Romano, N.; Becker, J. J.; Gagné, M. R. Inverting Pt-I Bond Polarization to Generate Iodonium Character. Under Review.

# **□** Recommended by ACS

# Preparation and Aromaticity of Rhenacycloprop-2-enecontaining Polycyclic Compounds

Liyan Zhan, Wei Bai, et al.

SEPTEMBER 21 2023

ORGANOMETALLICS

READ 2

# Inverting Pt-I Bond Polarization to Generate Iodonium Character

Kathleen R. Neff, Michel R. Gagné, et al.

AUGUST 11, 2023

ORGANOMETALLICS

READ **C** 

# Expanding the Utility of β-Diketiminate Ligands in Heavy **Group VI Chemistry of Molybdenum and Tungsten**

Daniel Leitner, Stephan Hohloch, et al.

JUNE 01, 2023

ORGANOMETALLICS

READ **C** 

## **Donor Strength Determination of Anionic Ligands**

Han Vinh Huynh, Truc Tien Lam, et al.

AUGUST 12, 2023

INORGANIC CHEMISTRY

READ **'** 

Get More Suggestions >